IEEE Access
Multidisciplinary | Rapid Review | Open Access Journal

Date of publication xxxx 00, 0000, date of current version xxxx 00, 0000.

Digital Object Identifier 10.1109/ACCESS.2017.Doi Number

Enhancing the response of a wearable sensor for improved respiratory rate (RR) monitoring

A. Ali[1], Y. Wei[1], Member, IEEE. J. Tyson[2], H. Akerman[3], A.I.R. Jackson[3,4], R. Lane[5], D. Spencer[2], N.M. White[2], Senior Member, IEEE.

[1]Smart Wearable Research Group, School of Science and Technology, Nottingham Trent University, NG11 8NS.
[2]School of Electronics & Computer Science, University of Southampton, UK, SO17 1BJ.
[3]Perioperative and Critical Care Theme, NIHR Southampton Biomedical Research Centre, University Hospital Southampton NHS Foundation Trust, Southampton, UK.
[4]Integrative Physiology and Critical Illness Group, Clinical and Experimental Sciences, Faculty of Medicine, University of Southampton, Southampton, UK
[5]Zelemiq Ltd, SP5 1EZ.

Corresponding author: A. Ali (e-mail: amjad.ali@ntu.ac.uk).

We would like to acknowledge and thank the National Institute for Health and Care Research (NIHR) funding support (NIHR202107) and the Nottingham Trent University Imaging Suite for support with microscopy imaging.

ABSTRACT: Currently available devices for monitoring respiratory rate (RR) are cumbersome and expensive (such as capnography and plethysmography), requiring skilled clinicians to operate and analyse. In contrast, the inexpensive and lightweight ones (e.g. reported strain, stretchable belt, and capacitive-based RR sensors) are unable to provide accurate RR measurements due to being highly affected by motion and environmental noise. This study aims to develop a wearable RR sensor with a high sensitivity and accuracy (comparable with capnography) of RR and which is not adversely affected by noise in comparison to other reported sensors in the literature. We have developed a flexible textile-based wearable RR sensor that can be conveniently embedded in a patient's gown. A design rule was adopted to empirically find the ratio of sensor electrodes with the aim to achieve the highest percentage output frequency change (%F.C). The empirical study also suggests that the %F.C can be further increased by increasing the dielectric material thickness between the sensor and ground electrodes. The enhanced textile-based sensor shows a 10.5% F.C toward the changes in the dielectric constant of a phantom, representing the human chest. The subsequent tests of the proposed RR sensor attached to the torso of the test subject shows a high-frequency variation (43 kHz) between crests (which corresponds to inhaling) and troughs (which corresponds to exhaling), with a 99.39% accuracy compared to the reported strain (a stretchable belt) and capacitive-based RR sensors. In the 35 performed RR tests, the proposed RR sensor picked up 495 crests; during the same tests, the capnograph showed a total of 498 respirations (which leads to 99.39% accuracy). This work demonstrates that the investigation in the electrode ratio and increase of dielectric layer thickness increases the proposed wearable textile base sensor %F.C, which leads to highly reliable (99.39% accuracy) RR detection with high-frequency variations and high SNR, as compared to gold standard capnograph, which is currently used in hospital for respiratory rate monitoring.

INDEX TERMS: Electronic textiles, Multi-layered screen-printed sensors, Respiratory rate sensor, sensors.

I. INTRODUCTION

Over 435 million people worldwide suffer from common chronic respiratory diseases, such as asthma, sleep apnoea, and chronic obstructive pulmonary disease (COPD) [1], [2]. On average, every year, four million people die prematurely from such chronic respiratory diseases [3], not to mention the medical costs estimated to be more than 50 billion dollars annually [4]. These numbers highlight the staggering magnitude of the global burden of lung health status monitoring and illustrate the critical need for an efficient and effective method to detect respiratory rates with non-invasive techniques.

Respiratory rate (RR) is a crucial parameter to monitor a patient's health, but it is still measured manually through breath counting. Unlike other essential parameters like heart rate, oxygen saturation (SpO2), and blood pressure, which are now measured automatically, manual breath counting requires significant staff time and may not be continuously monitored. Moreover, studies have shown that manual breath counting may not be accurate, and there are potential pitfalls associated with it. For instance, a retrospective study of 2.5 million nursing records observed a preference for RR of 14, 16, 18, and 20, which raises questions about the accuracy of manual breath counting [5]. Smaller studies have also demonstrated other probable inaccuracies in the manual recording of respiratory signs [5], [6]. Given the high resource utilisation and potential inaccuracies of manual breath counting, there is a need for accurate and reliable automated RR recording. The RR monitoring with capnography, plethysmography pulmonary function tests (PFTs) are highly accurate and treated as the gold standard in hospitals. However, they are expensive, need skilled clinicians to operate and are difficult to use in daily routine [7], [8][9].

A breath sensor and acoustic sensors are reported in [10], [11]. The breath sensor is located close to the nose and responds to the variation in flowing air's pressure, humidity, temperature, or carbon dioxide during breathing. An acoustic sensor reported in [11], this sensor is located on the neck and detects the acoustic sound produced at breathing time. The sensors located on the neck and near the nose could be highly precise. They can easily detect airflow as compared to those sensors located on the torso [12], which are more prone to walking, exercise, and arm movement artefacts. Although the sensors located near the nose and neck are highly precise, they are more noticeable and less comfortable as compared to those located on the torso. Optoelectronic plethysmography (OEP) is another standard method [13], [14], which uses cameras to monitor reflective markers placed on the patient's torso. The RR could be monitored by the relative movement of the reflective markers' 3D coordinates. However, the OEP method needs 20-to-54 reflective markers and 4-to-8 cameras [15], which is challenging to use in a daily routine. The RR, as mentioned above, sensors either directly measure RR or use surrogate markers. However, they have yet to be successfully integrated into widespread use in the healthcare market. These devices have limitations, such as requiring the patient to remain in certain positions or wear uncomfortable straps [14]-[20]. Additionally, some devices are plagued by inaccuracies, particularly in altered physiological states such as cardiac arrhythmia. The ultimate goal is to develop an accurate device that could monitor lung inflation and deflation with respiration, independent of other physiological variables, allows patients to move freely, and is non-invasive, along with having a medically acceptable standard value for accuracy of ±2 breaths per minute [21]. Unfortunately, such a device has not yet been released to the market.

Although a range of capacitive pressure sensors have been reported in the literature, such as: a textile-based capacitive pressure sensor that is taped to the abdomen to monitor movement due to respiration [22], [23], these sensors can be affected by other movements or unintentionally applied pressure. Another capacitive sensor, working on the pressure principle, is integrated into a textile-based mask that can monitor respiration [24]. However, the test subject needs to wear the face mask, which is uncomfortable to wear all day long.

Sarah et al. developed a compressible foam, encapsulated in non-stretchable textiles, whose resistance is changed when the pressure is applied [25]. It is wrapped around the torso to record chest expansion and contraction during breathing. However, the sensors may be uncomfortable and external forces could affect accuracy. Atalay et al [26] and Huang et al [27] developed strain sensors by weaving conductive fibers with non-conductive textile fibers. When the textile stretches, the contact area between the conductive fibers decreases, leading to increased resistance. However, the tight fit of resistive sensors around the torso can cause discomfort during extended use. A multimodal sensor embedded in a textile has been reported in [23]. The sensor could monitor multiple vital signs, such as elbow movements, thorax expansion and compression with breathing, and heart rate. Although this sensor could monitor multiple vital signs, the tight wrapping could be uncomfortable for a subject all day long. Additionally, the study missed the immense effect of noises, such as changes in humidity, temperature, vibrations, rubbing, bending, and pressure.

The research groups at Nottingham Trent University and the University of Southampton developed a novel textile-based RR sensor, working on the capaciflector principle, that can monitor the inhalation and exhalation of a human subject. The Capaciflector is the optimal choice for measuring respiration due to its ability to detect capacitance or electric field variations by sensing changes in the dielectric constant during the breathing. Unlike impedance-based and pressure-based sensors that require direct attachment to the body, the Capaciflector can

monitor respiration effectively when placed close to the body or integrated into clothing, ensuring non-invasive and comfortable continuous monitoring throughout the day. This innovative sensor technology is user-friendly, making it accessible for both patients and healthcare providers, and offers a cost-effective alternative to traditional devices like capnography and plethysmographs [7][28], which are cumbersome, require skilled operation, and are expensive. The Capaciflector's combination of non-invasiveness, comfort, ease of use, and affordability makes it the superior choice for respiratory monitoring, representing a significant advancement in the field. In the preceding work, a Capaciflector-based RR sensor was developed and attached to the torso of a test subject; the sensor actively monitors the lung's inflation and deflation with inhalation and exhalation, respectively [29]. During inhalation, the lungs are inflated, due to which a reduction in capacitance between the sensor electrode and lungs was recorded and vice versa, as shown in Figure 1. However, the initial sensor produced a maximum of 3.7 kHz frequency variation between crest and trough for each breath [29]. Although the sensor could accurately record the test subject's respiration, however, it has a low SNR of 2.43 due to the low %F.C. of 2.8 while considering the noise, motion artefact and environmental noise=1.15%. The %F.C. is calculated by measuring the sensor frequency variation with and without the presence of a phantom at 0.1 mm distance in front of the sensor, as represented by equation 1. 'SFP' stands for 'sensor Frequency in the presence of Phantom' and 'SF' stands for 'Sensor only Frequency'. Therefore, the current research aims to further increase the %F.C. along with the high SNR of the sensor and to reduce the impact of noise for better RR monitoring.

$$\%F.C=\frac{SFP-SF}{SF}x100 \qquad \text{(eq 1)}$$

It was hypothesised that the sensitivity toward RR monitoring could be further improved if the sensor sensitivity is further increased. One method to enhance the sensor sensitivity is to increase the electric field of the sensor electrode, resulting in a stronger capacitance between the sensor electrode and the object (alternatively, a high %F.C). This, in turn, results in higher sensitivity, as compared to the RR sensors reported in [1], [30], [31]. The development of design rules and an increase in dielectric material thickness were employed to enhance the RR sensor sensitivity of the previously reported wearable RR sensor [29]. Additionally, the proposed capaciflector-based sensor needs to be further investigated due to the following shortcomings in the currently reported RR sensors:

1. The proposed RR sensor monitors electric field/capacitance variations during breathing and does not undergo physical changes or disturbances, unlike other RR sensors reported in [1], [30], [31].
2. Due to this, the proposed RR sensor in this work does not have a limited life cycle for respiratory rate monitoring unless accidentally damaged, as compared to the RR sensors reported in [1], [30], [31].
3. Furthermore, the RR sensors reported in [1], [16], [17], obtain the RR information by comparing sensor data with its ideal conditions. This may lead to inaccurate monitoring, as it doesn't consider the effects of attachment and environmental factors like humidity and temperature.

This paper consists of five sections. Section two elaborates on the development of design rules. Section three explains the fabrication of the enhanced sensor. Section four details further sensitivity enhancement of the sensor and real-time respiratory rate monitoring (compared to capnography respiratory rate detection) of a test subject. Finally, the article concludes in section five.

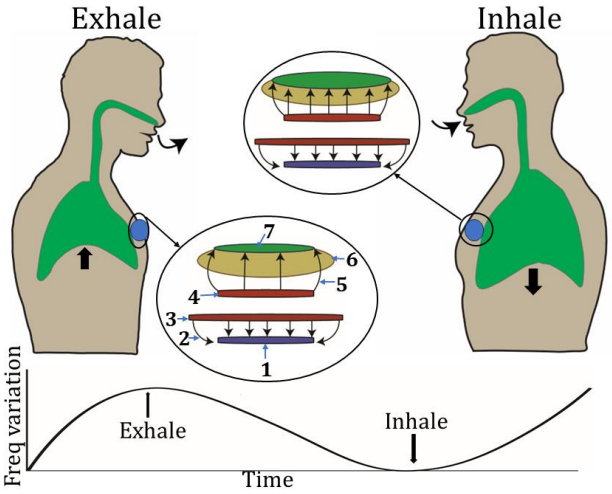

FIGURE 1. Schematic of the sensor setup for monitoring the respiratory rate of a test subject's exhalation and inhalation. Where 1 represents the ground electrode, 2 represents the electric field between the ground and reflector electrode, 3 represents the reflector electrode, 4 represents the sensor electrode, 5 represents the electric field between the sensor electrode and test subject torso, 6 represents body tissue and bones, and 7 represents covered lungs area.

II. DEVELOPING A DESIGN RULE TO ENHANCE THE % F.C OF THE WEARABLE RR SENSOR

The proposed wearable (textile-based) RR sensor geometry consists of three electrodes separated by a dielectric material; the whole system is known as a capaciflector, which has been previously reported in [29][32] and also elaborated in supplementary data. The first electrode is grounded and referred to as the ground electrode, shown in Figure 1, denoted by number 1. The second and third electrodes are set to the same voltage of 3 volts and are known as the reflector and sensor electrodes, respectively, as shown in Figure 1, denoted by numbers 3 and 4. The reflector electrode generates a strong electric field and high capacitance with the ground electrode, denoted by number 2. Simultaneously, it reflects most of the electric fields from the sensor electrode towards an object to be sensed, denoted by the number 5. Consequently, the sensor

electrode creates an electric field and capacitance with nearby objects, known as Cso, as depicted in Figure 1, denoted by number 5. Additionally, Figure 1 shows how the electric field between the sensor electrode and the lungs decreased and increased with exhalation and inhalation, respectively (which is due to the smaller and larger lungs-covered area by the sensor during exhalation and inhalation). However, even with the presence of a reflector electrode, a small portion of the electric fields (fringing field effect) are still attracted by the ground electrode, forming a capacitance referred to as Csg, as shown in the electrical circuit configuration in Figure 2. Therefore, according to equation 2, which is the total capacitance (Ct) of the sensor electrode, decreasing Csg while increasing Cso leads to enhanced sensor sensitivity [33].

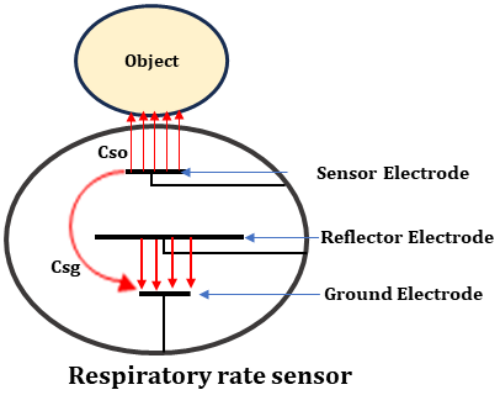

FIGURE 2. The equivalent circuit model of the respiratory rate sensor's interfacing circuit.

$$Ct=Csg+Cso \qquad \text{(eq 2)}$$

The detailed simulations, manufacturing, and fundamental testing of the proposed sensor are reported in the previous work [29]. This paper describes a method of enhancing the sensor response for robust respiratory rate monitoring while keeping the sensor size as small as possible. In this work, the flexible copper tape was cut in a circular shape using a Roland GS-24 vinyl cutter [33], [34]. The ratio between three electrodes, sensor, reflector and ground, varies from 1:1:1 to 5:5:5, with multiples of 8. For instance, a 1:1:1 ratio corresponds to 8:8:8 mm diameters for the sensor, reflector, and ground electrode, respectively (alternatively, each electrode has a diameter of 8mm, while the thickness is standard 90 microns). In case the ratio size is increased, such as 2:2:2, then each electrode diameter will become 16mm, as 8 is the basic multiplier. A 2.5 cm wire was soldered to each electrode for connectivity with the interfacing circuit, as depicted in Figure 3, where the interfacing circuit, DAQ card and data processing are elaborated in the preceding work [29], (also could be found in the supplementary data). In total, there are 125 ratio combinations. Therefore, instead of developing a new screen for each ratio combination, copper tape was used (described above) to reduce the cost and carbon footprint. The objective of this study is to experimentally validate the best performance using different ratios in comparison to a water phantom, which mimics the human body's lungs (as 80% of the human lungs consist of water [35]). To study all 125 combinations and find the best ratio that has the highest sensitivity, the following design rules were established, shown in Figure 4- flow chart.

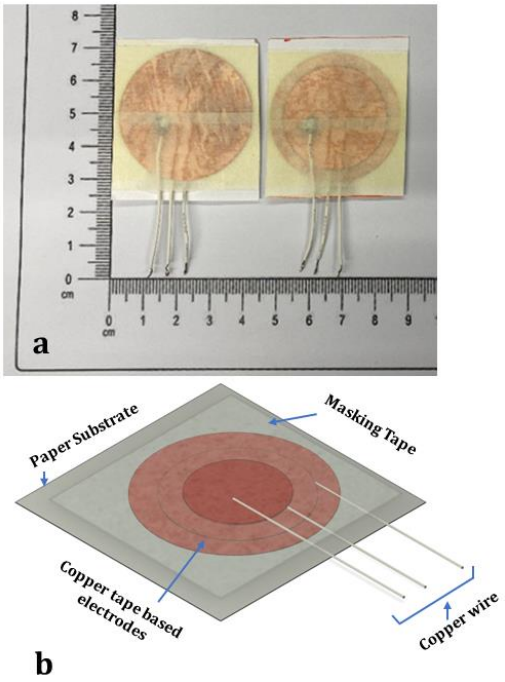

FIGURE 3. The sensor was created using flexible copper tape, dielectric masking tape, and wire for electrode connection. The three-electrode ratio combinations are: a) 5:5:1 and 4:5:1. b) 3D layout of copper tape-based sensor.

Rule 1: The reflector must be greater than or equal to either the sensor or the ground electrode.

This ensures that the sensor electrode's maximum electric fields are directed towards the phantom (otherwise, the sensor electric field would be attracted towards the ground electrode), resulting in a strong capacitance with the phantom and a higher percentage frequency change (%F.C). Following this rule, 55 combinations (e.g., 5:1:5) with smaller reflectors were excluded. The design rule is also demonstrated with the help of a flow chart, shown in Figure 4.

Rule 2: A minimum threshold of a 10% frequency change.

The remaining 70 combinations were fabricated using flexible copper tape with paper as substrate and masking tape as the dielectric layer for separation. The 70 manufactured sensors were then empirically tested against the water phantom. Based on empirical data, the %F.C -

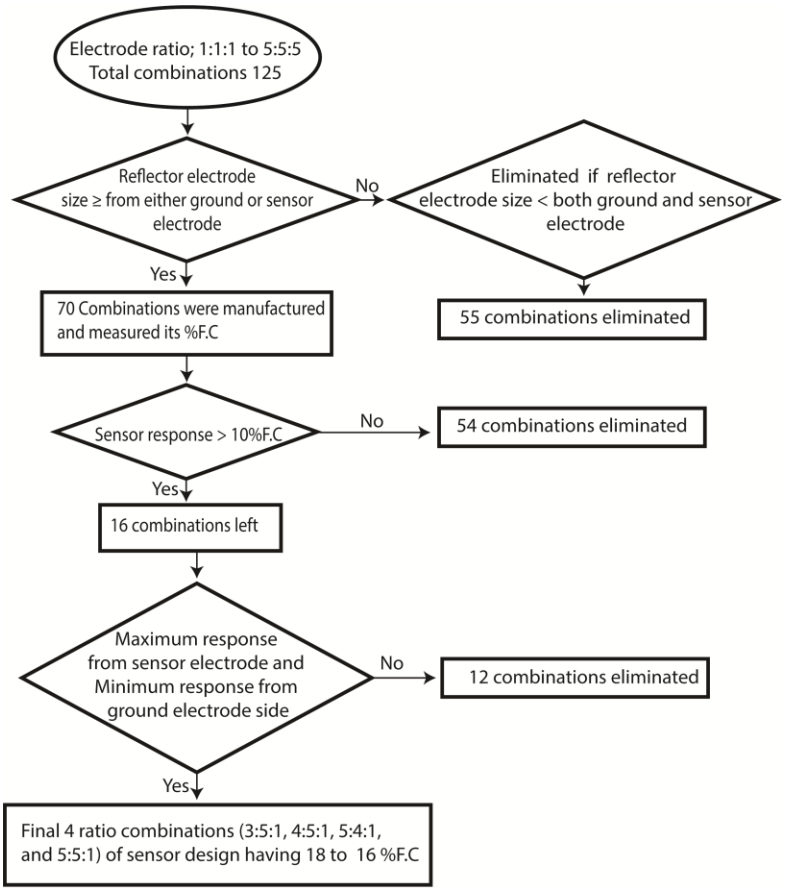

FIGURE 4. **Flow chart of the Design rule for eliminating that electrode combination that either has a smaller %F.C from the sensor electrode side or has an active moderate sensitivity from the ground electrode side.**

-ranges from 1.5 to 18.2% for 70 sensor combinations. Figure 5 illustrates how the % F.C. varies among different sensor ratio combinations, with the examples of 2:4:5, 4:5:1, 5:5:1, 5:4:1, and 3:5:1. The sensor pool is big (70 combinations), and the % F.C. ranges from 1.5 to 18.2%. Therefore, a minimum 10 %FC threshold was set to rule out sensor designs with lower %F.C. Based on these criteria, 54 combinations were ruled out, resulting in 16 combinations left.

Rule 3: Maximising the response from the sensor electrode and minimising the response from the ground electrode.

At this stage, it was essential to consider the backside response of the remaining 16 combinations. As an RR sensor, it should have minimal sensitivity from the side of the ground electrode to be immune to other moving objects nearby. On the other hand, it should have maximum sensitivity from the side sensor electrode to maximise sensitivity towards lung inflation and deflation. Thus, 12 combinations were removed due to a high or moderate sensitivity from the side ground electrode compared to the sensitivity from the sensor electrode. Thus, only four designs: 3:5:1, 4:5:1, 5:4:1, and 5:5:1 are left. These designs produced %F.C of 18.1%, 17%, 16.5%, and 16.3% from the sensor electrode side, respectively. Additionally, it was ensured that four ratio combinations had minimal %F.C responses from the ground electrode (backwards), measuring 2.6%, 1.6%, 1.9%, and 1.6%, respectively.

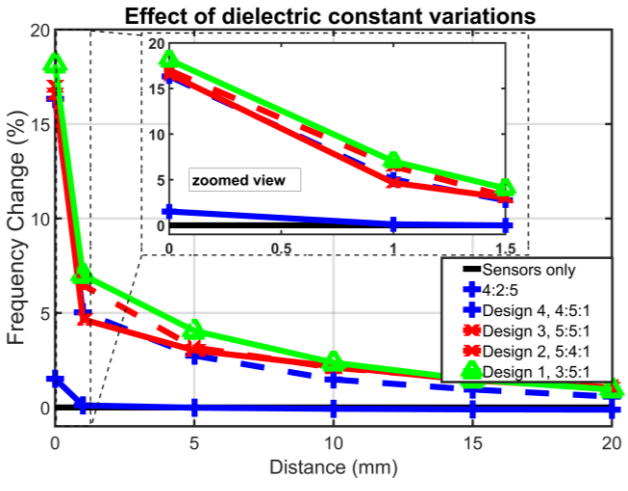

FIGURE 5. **Using the design rule, the best design (3:5:1) with 18.2% F.C is compared to the (2:4:5) design with a minimal 1.5% F.C. The zoomed view shows sensor sensitivity at 0mm (sensor touching phantom) and at 1mm.**

III. SCREEN PRINTING OF RESPIRATORY RATE SENSOR ON WEARABLE TEXTILE

The next task is to transfer the empirically tested copper-tape-based sensor combinations having a high %F.C of 18.1 to textile-based sensors. For this purpose, the screen-printing mechanism is employed, as reported in the preceding work [29]. In the production of the wearable sensor, we utilised polyester/cotton fabric (50%/50%) that was screen printed. This fabric is similar in composition to the fabric used in hospital patient gowns, making it the most suitable option for the specific application being studied [36]. Silver ink received from Henkel was used to manufacture the conductive electrodes of the sensor instead of using flexible copper tape. These conductive electrodes are separated using UV-curable dielectric polymer ink from Electra Polymers Ltd, which acts as the interface, dielectric layers, and encapsulation. Initially, a UV-curable dielectric ink layer was developed to act as an interface layer, which is cured in a UV conveyor for 20 seconds. This layer provides a smooth surface for the subsequent printing of the silver layer. Then, a silver layer, referred to as a ground electrode, is deposited and cured at 120℃ for 10 minutes. However, the drawbacks of this mechanism are that it is highly time-consuming (taking 8 hours to create the UV-curable dielectric ink interface layer) and also increases the rigidity of the sensor.

A. PU Vinyl

To reduce the manufacturing time and improve the flexibility and bendability of the sensor, a vinyl sheet is used. A range of vinyl sheets with varying materials were considered and tested to investigate a suitable one that can be used as a replacement for the screen-printed dielectric -interface layer. Initially, Polyurethane vinyl (PU vinyl) was considered. The PU vinyl was laminated on fabric using a heat press at 130 ºC for 15 seconds. If the vinyl adhesive is not properly fused with the fabric, then there is a chance of peeling off the vinyl from the fabric and potentially damaging the textile-based RR sensor. Therefore, the heat press process was repeated three times to fuse the vinyl adhesiveness with the fabric properly. A crude test was made to deposit the silver ink on a prepared PU vinyl. However, it started chemical reactions, as shown in Figure 6-a, which was not desirable and potentially damaged the sensor structure.

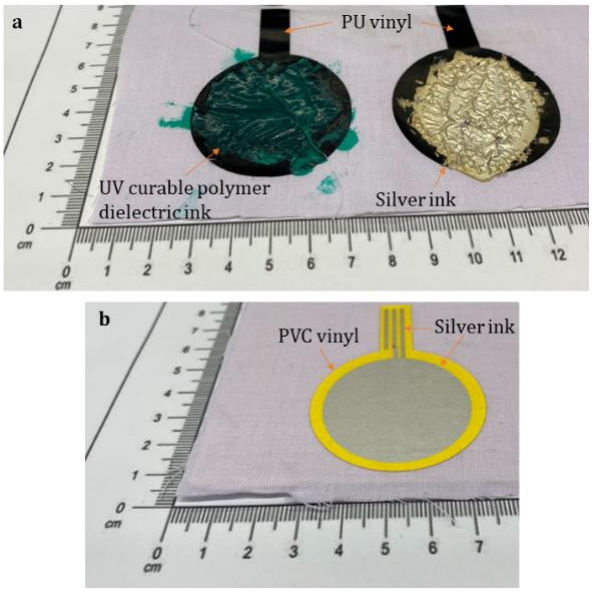

FIGURE 6. a) PU vinyl chemically reacts with UV-curable polymer ink and silver ink. b) silver ink is pasted on PVC vinyl, which is not reacting.

B. PVC Vinyl

A thermal transfer Polyvinyl Chloride (PVC) vinyl sheet was found to provide the best interaction, as other vinyl sheets (PU vinyl) reacted with the screen-printed silver layers, introducing roughness and oxidation between the layers that prevented the continuity of each electrode, as shown in Figure 6 a-&-b.

The introduction of the vinyl sheet helps to reduce the printing time of the interface layer from 8 hours to 2 minutes, provides a comparatively smooth surface for subsequent printing, and increases flexibility through a reduced overall thickness of 0.18mm (a 28% reduction from 0.64mm). The introduction of vinyl also contributes to the recyclability of textiles and the sensor. The entire sensor can be peeled off from the fabric by applying an adhesive removal spray on the fabric side, which will lose adhesiveness and can be peeled off the sensor part from the textile.

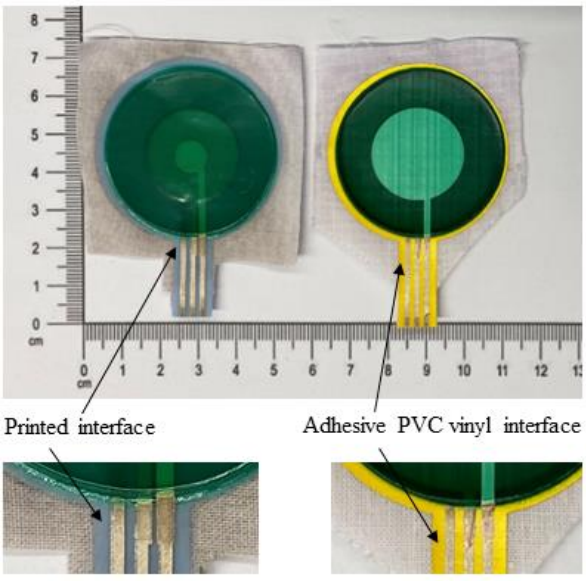

FIGURE 7. Screen printed interface layer vs Laminating adhesive PVC Vinyl on Fabric with the help of a heat press to use as an interface layer.

The final screen-printed sensor with an interface layer (a screen-printed dielectric ink) and PVC vinyl is shown in Figure 7.

IV. RESULTS AND DISCUSSION

In the sensor design, a range of crucial factors were considered to enhance the sensor's response toward phantom movement, which closely mimics the human body, as elaborated in supplementary data and in the previous work [29]. These critical factors include the conductivity and resistivity of electrodes, the depth of the dielectric materials used between electrodes, and the types of dielectric materials used for insulation and encapsulation.

After each silver print, the sensor is cured at 120 °C in the oven for 10 minutes. To produce the first batch of textile-based sensors having new combinations of 3:5:1, 4:5:1, 5:4:1, and 5:5:1, the conductive layers are printed with one print, the dielectrics with two prints, and the encapsulation with one print (smaller the number of prints leads to thinner layer).

A. Thickness impact on sensor %F.C

The experimental testing procedure for the suggested sensor has been explained in the previous study [29], also elaborated in supplementary data. The same experimental testing procedure was employed to measure the % F.C toward water phantom of the textiles-based new printed combinations (3:5:1, 4:5:1, 5:4:1, and 5:5:1). Surprisingly, these textile-based sensors do not produce a high % F.C (1.67%) compared to the same design made of copper tape (18%F.C). After critically analysing both types of sensors (manufactured with copper tape and screen printed on textile), the significant differences noticed are the thickness of dielectric material between the sensor and ground electrodes and its type (masking tape vs screen-printed UV curable polymer ink). Although, the connectivity test on a multimeter shows similar results between two distant points (3 cm apart), with a resistance of 1.5 Ω for the cured silver and 0.2 Ω for the copper sheet.

A hypothesis was formulated that the dielectric constant and thickness of the dielectric material are potential parameters that could increase the percentage frequency change (%F.C). Because the dielectric constant (or relative permittivity) of a material indicates its ability to store electrical energy in an electric field [37]. A higher dielectric constant results in greater capacitance in a capacitive sensor. Additionally, the thickness of the dielectric material significantly impacts the sensor's capacitance. According to the capacitance equation 3:

$$C=\frac{\epsilon r \epsilon . A}{d} \qquad \text{(eq 3)}$$

In equation 3, ‘ϵr’ denotes the dielectric constant of the added material, ‘ϵ.’ represents the permittivity of free space, ‘A’ stands for the area of the capacitor plates, and ‘d’ is the thickness of the dielectric material. In most cases, a thicker dielectric layer (increased 'd’) will decrease the capacitance, all other factors being constant. However, a strategic optimisation of the dielectric layer thickness between the sensor and reflector, and between the reflector and ground, relative to the dielectric constant and electrode configuration, significantly enhances sensor electrode sensitivity toward the intruding object, consequently impacting the %F.C.

To test this hypothesis, the dielectric material thickness between the sensor and ground electrodes progressively increased by adding more prints— such as two prints, four prints, eight prints, and 16 prints. Scanning electron microscopy (SEM) was used to measure the thickness of the dielectric material. Figure 8 shows the sensors with 2 and 16 prints for the dielectric layer. It also shows how the thickness was increased from 20 µm to 265 µm with increasing in the number of prints. Figure 9 and Table 1 report the increase in the thickness of the dielectric layer with an increase in the number of prints. The thickness measurements in Table 1 exhibit an average 8% variation in the same design, number of prints, and number of deposits. The % F.C. of each printed version sensor was measured toward the water phantom, as elaborated in the supplementary date, and in the preceding work [29]. Figure 10 demonstrates that in the absence of the phantom, all sensors exhibit 0 percentage frequency change (%F.C), indicating no impact on their response.

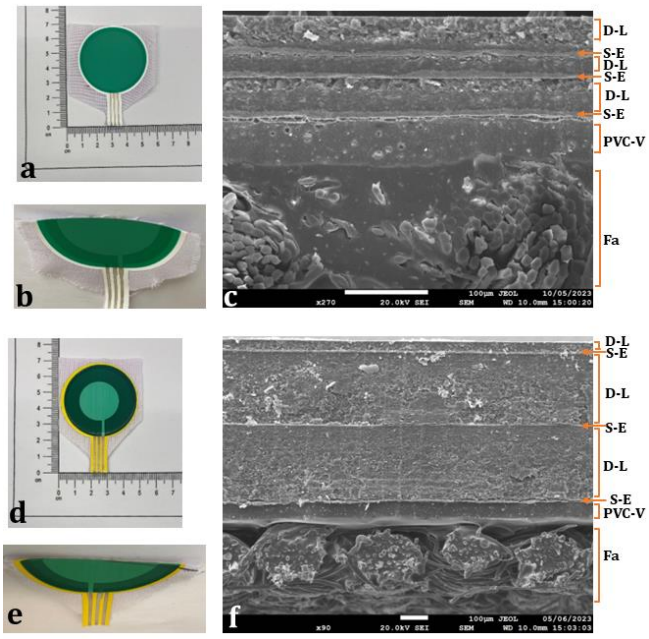

FIGURE 8. The comparison of two batches of Design 1(3:5:1), one has 2, and the second has 16 screen prints between the ground and reflector and between the reflector and sensor electrode, shown in a & d, respectively. Both sensors were cut in half (as shown in b and e) for SEM cross-sectional analysis of each layer thickness (as shown in c and f). Fa stands for fabrics, PVC-V stands for PVC vinyl, S-E stands for silver electrode, D-L stands for dielectric layer.

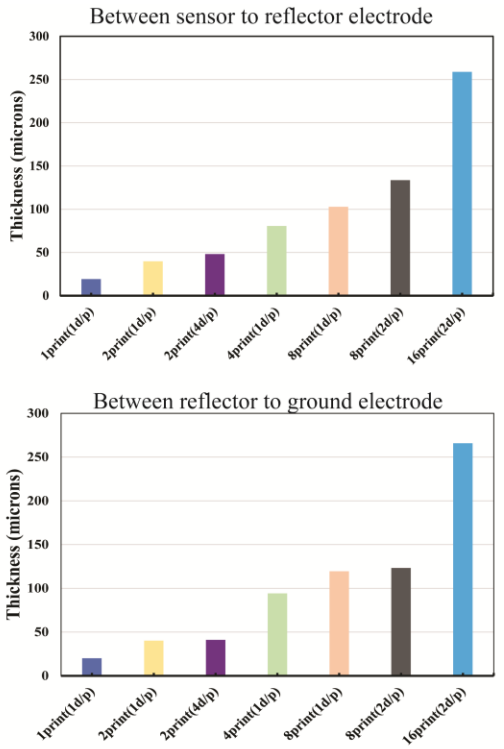

FIGURE 9. Increasing dielectric layer thickness with an increasing number of screen prints between sensor to reflector and reflector to a ground electrode.

ABLE 1.
SEM WAS USED TO MEASURE THE THICKNESS OF THE DIELECTRIC MATERIAL IN DESIGN 1, WHICH WAS SCREEN-PRINTED WITH A PROGRESSIVELY INCREASING NUMBER OF PRINTS AND DEPOSITS PER PRINT. THE OVERALL SENSOR THICKNESS AND THEIR CORRESPONDING %F.C., (Y_D/P) STANDS FOR Y_DEPOSITS/PRINTS.

Design 1, X_Prints (Y_d/p)	Thickness between sensor to reflector (µm)	Thickness between reflector to ground (µm)	Overall sensor thickness (µm)	%F.C
Design 1, 1_print (1d/p)	19	20	372.8	1.4
Design 1, 2_prints (1d/p)	39.7	40	419.6	11.6
Design 1, 2_prints (4d/p)	48.2	41	431.4	11.8
Design 1, 4_prints (1d/p)	80.7	94.2	531.3	88.2
Design 1, 8_prints (1d/p)	102.8	119.5	576.8	99.1
Design 1, 8_prints (2d/p)	133.6	123.2	582.4	9.2
Design 1, 16_prints (2d/p)	258.8	265.8	889.2	10.5

However, when a water phantom is introduced nearby, a variation in the dielectric constant occurs, which is monitored by the sensor in the form of an abrupt change in the sensor %F.C. Each sensor shows a maximum %F.C at 0mm, indicating physical contact with the phantom. In the second step, the phantom is located at 1 mm from the sensor to observe the sensor's response without physical contact. In this case, the sensor %F.C is reduced by 0.5, which shows that the sensor accurately monitors the change in the surrounding dielectric constant. Additionally, the progressively increasing number of screen prints has a significant impact on the sensitivity. The sensor with the same design (3:5:1) but an increased number of prints, 16 prints (2 deposits per print), shows a 10.5 %F.C compared to the 1.4 %F.C of the same sensor design (3:5:1) with one print (1 deposit per print), shown in Figure 10. This represents a 7.5-fold increase in sensor response by increasing the thickness of the dielectric layer from 39/(40) microns to 258.8/(265.8) microns. Table 1 further elaborates on the overall thickness and measured %F.C at 0mm distance against the water phantom. The empirical comparison of the design-1 sensor, manufactured with adhesive copper tape, and the screen-printed wearable sensor shows that the %F.C. exhibits a more linear pattern in the case of wearable sensors. On the other hand, the sensor manufactured with copper tape exhibits an abrupt %F.C change of 10.5% in the distance range of 0 to 1mm. This abrupt pattern is similar for other designs as well in the case of copper tape-based sensors.

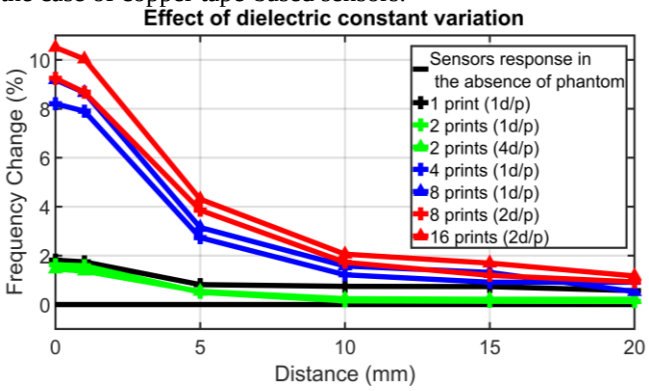

FIGURE 10. Empirical analysis of the number of screen prints impact on sensor response towards water phantom. d: deposit, p: prints.

B. Environmental noise impact on the proposed sensor

In our earlier work [29], various types of noise that could potentially affect sensor response, which could potentially lead to false respiratory rate monitoring, were examined. The types of noise analysed in earlier work (also elaborated in supplementary data) include motion artefacts, such as bending, rubbing, and pressure, as well as environmental noise, such as temperature and humidity variations. The earlier reported analysis revealed that the sensor is

significantly affected by environmental noise, particularly temperature and humidity variations. The best design (Design 2) maximum response towards the phantom was 2.8%F.C. However, temperature and humidity changes cause 1.15%F.C collectively [29]. Although 2.8%F.C was higher than 1.15 % F.C., other sources of noise, such as motion noise, can make it even higher, potentially leading to false respiratory rate readings.

This work aims to increase the sensor's %F.C. while minimising the impact of temperature and humidity variations. However, in reality, it is challenging to eliminate the influence of temperature and humidity variations entirely. The % F.C of the sensor with 16 prints (2 deposit/ print) was measured toward the dielectric constant variations (occurred due to the water phantom moving away) in an environmental control chamber, where the temperature was raised from 15 ºC to 35 ºC at a fixed relative humidity of 60 %RH, as shown in Figure 11. Figure 11 demonstrates an average standard deviation of 0.68 in the %F.C across all tested temperature points (15 ºC, 25 ºC, and then 35 ºC). A similar experiment was conducted where humidity varied from 40 %RH to 80 %RH while maintaining a constant temperature of 24 °C, as also shown in Figure 11. Similarly, Figure 11 shows that a 40% relative humidity increase resulted in an average standard deviation of 0.36 in the sensor's %F.C. Table 2 presents the %F.C. in the presence of a phantom. The signal-to-noise ratio (SNR) of each design was calculated and then summarised in Table 2. Version 1, the best design (Design 2), could accurately measure the respiratory rate with a 98.68% accuracy despite having a lower SNR of 2.43, reported in previous work [29]. In this work, version 2, Design 1 with 16 prints (2 deposit/print) achieved a further increase in SNR to 10.09, which is four times higher than the previous design, which also further increased the accuracy to 99.39% (The accuracy calculation is given in the supplementary data), where the respiratory rate experiments are given below.

TABLE 2.
THE SIGNAL-TO-NOISE RATIO (SNR) OF VERSION 1 SENSORS WAS PREVIOUSLY REPORTED IN [29], AND VERSION 2 SENSORS. (D/P) STANDS FOR (DEPOSIT/PRINT).

Parameter	Version 1, Design 2	Version 2, Design 1, 16 prints (2 d/p)
%F.C	2.8	10.5
Impact of humidity	0.2	0.36
Impact of Temperature	0.95	0.68
SNR	2.43	10.09

C. Proposed sensor repeatability

To test the proposed RR sensor's repeatability capability, five different batches of Design 1 (same design) were screen-printed to produce five identical sensors of Design 1, as shown in Figure 12-a. In these five batches, the only difference is different batches; the rest of the design parameters are identical, such as electrode ratios,

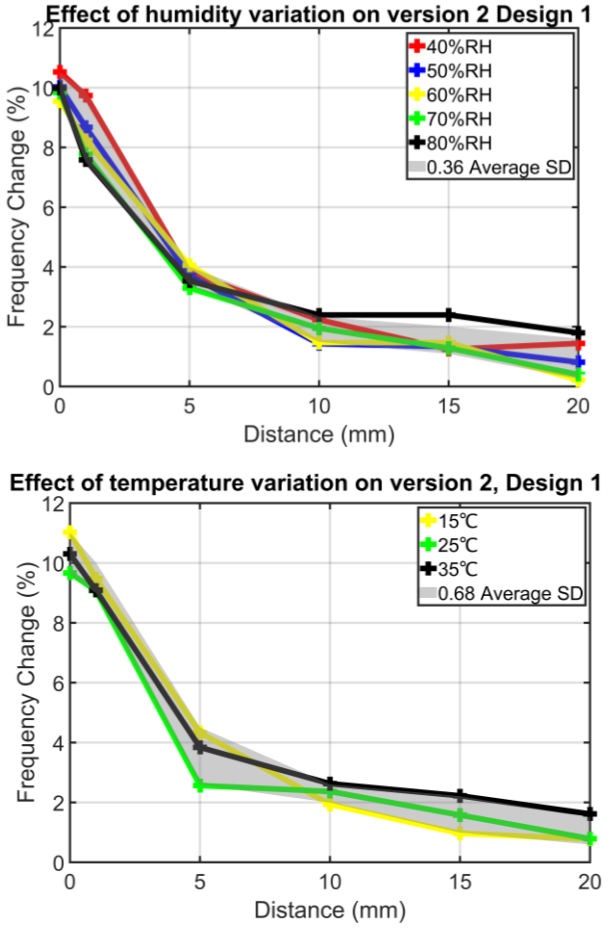

FIGURE 11. Humidity and temperature variation impact on the sensor %F.C, SD stands for standard deviation.

-the geometry of each layer, the position of each layer in the sensor design, and the number of screen prints of each layer (alternatively thickness). The % F.C. toward the water phantom of each printed identical sensor (Design 1) from five different batches was measured, as elaborated above in section IV-A. The measured % F.C. of five identical sensors (from different batches) was drawn, shown in Figure 12-b. The comparison of five identical sensors of Desing 1 shows that Design 1 from each batch has a higher %F.C of 10.5, with a maximum of 0.1 standard deviations. The analyses of these empirical results show that the proposed sensor has the repeatability capability.

D. Respiratory rate monitoring

It is hypothesised that the increase in %F.C. of the proposed sensor would better monitor lung inflation (due to breath inhalation) and deflation (due to breath exhalation). In the previous work [29], it was found that the version 1 proposed sensor (Desing 2) had clear and precise respiratory rate monitoring capability when attached to the torso at the bottom end of the sternum bone (also known as position 8), shown in Figure 13-a-

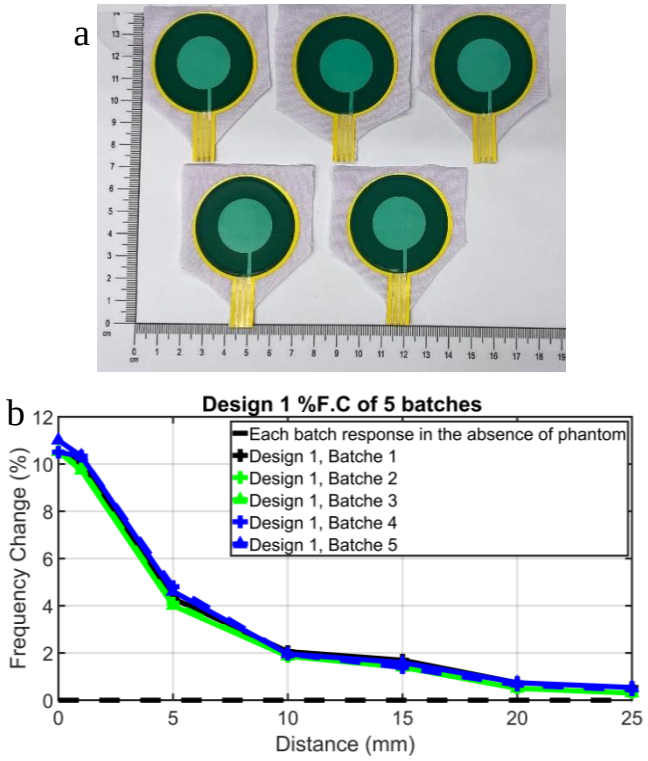

FIGURE 12. a) Identical five replicas of Desing 1 (electrode ratios 3:5:1) from five different batches of screen printed. b) Comparison of the measured %F.C. of five identical sensors (from five different batches) of Desing 1.

-(A consent for publishing the data has been obtained from the test subject). Although the respiratory rate has been precisely encoded in the form of frequency variation with troughs (corresponding to exhalation) and crests (corresponding to inhalation), however, the high-frequency variations due to exhalation and inhalation are more desirable, as they will be less affected by noise and will precisely and accurately record the respiratory rate of a test subject. Where the best sensor (Design 2) of version 1 shows a 3.7 kHz maximum frequency variation with inhalation and exhalations. The improved sensor in this work, having 16 prints, which shows a high %F.C. (10.5) towards changes in the surrounding dielectric constant, was attached to position eight on the torso of the test subject as elaborated in the preceding work [29]. The test subject was wearing a capnograph mask (Creative PC-900B), which is the gold standard for respiratory rate monitoring applications [28].

The capnograph recorded 14 breaths, whilst the sensor recorded data showing 14 highly precise crests. The analysis of version 2, Design 1, response toward breathing shows a maximum of 43 kHz frequency variation, which is a 12.7-fold improvement as compared to version 1's most sensitive sensor, Design 2 (3.7 kHz).

To test the sensor repeatability, accuracy, and reliability, the respiratory rate experiment for position eight on the torso elaborated above was conducted on different days, continuously for 20 days, such as Day 1, Day 2…., and Day 20. The version 2 sensor consistently records the respiratory rate with high-frequency variations (ranging from 38 to 43 kHz), as shown in Figure 13-b. In each experiment, the capnograph-recorded respiratory rate was used as a gold standard for reference.

To test the proposed sensor repeatability capability, five identical sensors (from different batches) of Design 1 (the same design) were screen printed as elaborated in sections IV-B and C, and shown in Figure 12-a. These five identical sensors of Design 1 were attached one by one to position 8 of the test subject's torso and recorded the test subject's breathing as elaborated above, along with the test subject's wearing the capnograph mask. Figure 14 shows that the identical sensors (Design 1) from different batches can actively record the respiratory rate of a test subject in the form of frequency variation (with 43 kHz maximum and 23 kHz minimum frequency variations). Additionally, it has been observed in Figure 13-b and Figure 14 that the sensor does not follow a single frequency baseline since the principle of the sensor is to detect frequency variations (alternatively capacitance variations) associated with breathing rather than a single frequency, making the baseline frequency irrelevant. However, the number of picked-up crests by the proposed RR sensor exactly matched the capnograph-recorded number of respirations. Furthermore, it has been noticed in Figure 14, that identical sensor designs (Design 1) from five different batches produced a maximum of 41, 25, 34, 27, and 30 kHz with breath inhaling and exhaling; these differences in maximum frequency variations are most probably due to un-noticeable differences in sensor attachment to the torso and deep, normal, or shallow breaths taken by the test subject. However, the average frequency variations due to breaths inhaling and exhaling across all identical sensors from five different batches is 25 kHz. Furthermore, the preceding work reported in [29][32], demonstrated that the proposed sensor is capable of monitoring a test subject's respiratory rate while standing and walking. The details can be found in the supplementary data.

E. Proposed sensor comparison with reported literature

Since the proposed sensor works by monitoring the electric field/ capacitance variations between the sensor and inflating/ deflating lungs during breathing, the sensor itself does not undergo any physical changes or disturbances. Therefore, the proposed sensor does not have any time limitations or a limited life cycle toward respiratory rate monitoring until it has been accidentally damaged, unlike reported capacitive, stretchable belt, and strain sensors mentioned in [1], [30], [31]. Since their lifespan depends on the maximum number the capacitive/stretchable belt or strain sensor can withstand under applied pressure or stress.

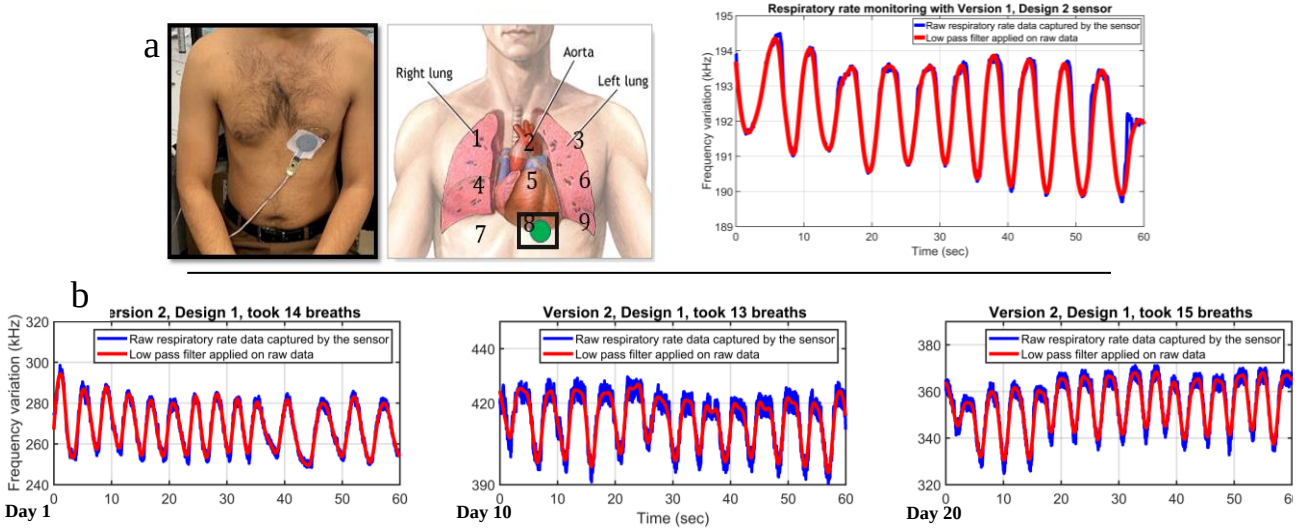

FIGURE 13. **a) In version 1, the Design 2 sensor picks up 11 crests with the corresponding 11 respiration recorded on the capnograph; the maximum frequency variation is 3.7 kHz. b) The improved sensor with 16 prints, also known as version 2 Design 1, is attached at position 8, where the sensor picked up 14, 13, and 15 precise crests with a maximum 43 kHz frequency variation with the corresponding 14,13 and 15 respiration recorded on the capnograph, respectively.**

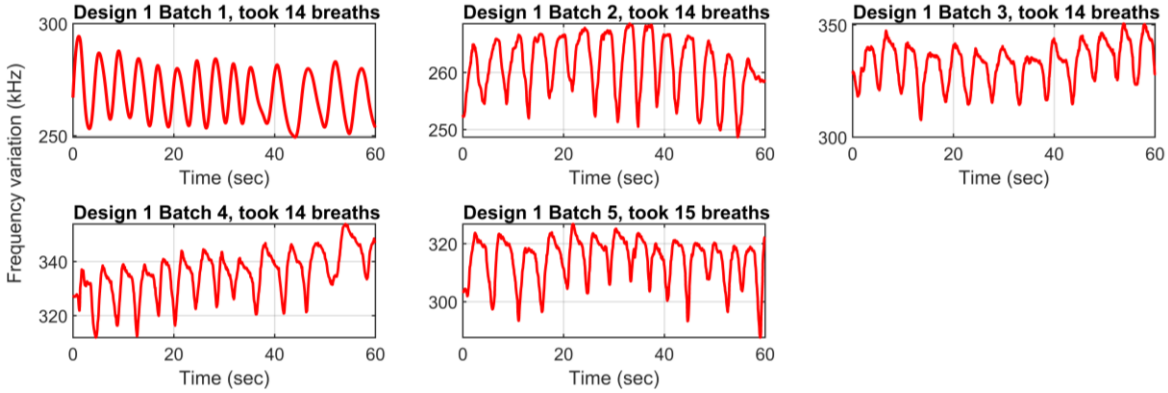

FIGURE 14. **Comparison of the respiratory rate (RR) test by using identical sensors of Desing 1 from five different batches. Breath inhaling and exhaling cause a maximum frequency variation (FV) of 41, 25, 34, 27, and 30 kHz by Batch 1, 2, 3, 4, and 5, respectively. The average FV across all five identical sensors is 25 kHz.**

TABLE 3.

THE PROPOSED RESPIRATORY RATE SENSOR COMPARISON WITH THE TO-DATE REPORTED RESPIRATORY RATE SENSORS. F, R, V, I, AND C STAND FOR FREQUENCY, RESISTANCE, VOLTAGE, CURRENT, AND CAPACITANCE.

References	Printable on Textile	Sensor mounting position	Monitoring parameter	Pre-Calibration required	Sensing mechanism	Impact of Environmental and Motion Noise	Measurement accuracy	Max F, R, V, I, C variation with respiration
[20]	No	Wrap around chest	Chest expansion	Yes	Strain based	Not given	Not given	R=0.98 Ω
[25], [39]	No	Mounted on torso	Chest applied pressure	Yes	Resistive based	Not given	Not given	R=2 to 4 kΩ
[40]	No	Distant monitoring	Thorax movement	Yes	Capacitive based	Not given	Not given	ΔC=0.02%
[23]	No	Wrap around chest	Thorax movement	Yes	Capacitive based	Not given	Not given	ΔV=0.02 v
Preceding work [29]	Yes	Anywhere on torso	Lung inflation and deflation	No	Capacitive sensing (capaciflector)	Sensor response 2.4-fold > sum of all noise.	98.68%	F =3.7 kHz
This work	Yes	Position 8, shown in Figure 13-a	Lung inflation and deflation	No	Capacitive sensing (capaciflector)	Sensor response 10-fold > sum environmental noise	99.39%	F=43 kHz

Additionally, as mentioned above, the proposed sensor monitors variations in the electric field, so lifting off or becoming loose does not have a crucial impact on respiratory rate monitoring. In the worst-case scenario, the sensor may incorrectly record or miss a breath if it becomes loose or is lifted off, as long as the sensor stays within the 5mm range. A change in frequency was observed when the sensor became loose; however, after becoming loose, it resumed monitoring respiration with frequency variation on the shifted baseline (this shifted baseline corresponds to the degree of losing). In contrast, the sensor reported in [1], [30], [31] will lead to complete inaccuracies or may not monitor the respiratory rate at all if the reported sensor in [1], [30], [31] becomes loose or is lifted off.

RR sensors reported in [1], [16], [17] obtain the RR information by comparing the sensor data with itself when the sensor is in ideal conditions (not attached to the test subject), which could lead to inaccurate respiratory rate monitoring, as it fails to account for the effects of attachment (such as using belt or adhesive) and environmental factors such as humidity and temperature variations. Further, a detailed comparison with the recently reported literature is given in Table 3.

Although the initial test of the proposed sensor shows a good proof of concept, this study has some limitations. The study is being performed on a small, homogeneous group of healthy individuals. Further studies are needed on a heterogeneous population, including healthy people of diverse age ranges, hospitalised patients of different ages, and more practical daily routines.

V. Conclusion

A new design rule has been developed to identify the optimal ratio combinations of electrodes for the most sensitive respiratory rate (RR) capaciflector-based sensor, out of a pool of 125 possible combinations. Furthermore, With the support of the design rule, the sensor sensitivity toward water phantom has been increased by 3.7-fold compared to the team's previous design (version 1 sensors). The selected four designs were transformed into textile-based sensors. It was also empirically discovered that the sensitivity of the proposed textile-based sensors can increase with an increase in the dielectric material thickness. This improvement enhances the proposed sensor SNR from 2.43 to 10.09 compared to the previous versions of the sensor. This leads to high-frequency variations (43 kHz) between inhaling and exhaling breaths. More than 35 RR tests were performed, where the number of picked-up crests by the proposed RR sensor was 3 less (495 crests) than the capnograph-recorded number of respirations (498 respirations). The sensor was validated by attaching it to the torso of a test subject, which precisely records the respiratory rate with 99.39% accuracy. Furthermore, the proposed sensor has the repeatability capability, where the identical sensors from different batches show similar %F.C. and RR detection. Additionally, the proposed sensor monitors the RR by monitoring the change in dielectric variations with inhaling and exhaling breath and does not pass through physical changes (such as strain and compressible capacitive RR sensors, which undergo strain and pressure) while monitoring respiratory rate.

Future work: This study has successfully laid the groundwork for sensor development, sensitivity enhancements, impact of environmental noise, and real-time testing on a single test subject. However, future work will focus on embedding the sensors into hospital garments, ensuring they can adapt to body movements while maintaining accuracy, conducting washability tests, and testing on a heterogeneous population, including healthy individuals of diverse age ranges, hospitalised patients of different ages, and under more practical daily routines.

ACKNOWLEDGMENT

We would like to acknowledge and thank the National Institute for Health and Care Research (NIHR) team for their funding of this Invention for Innovation (i4i) project (NIHR202107) and the Nottingham Trent University Imaging Suite for support with microscopy imaging. An AI tool (Grammarly) is used for text grammar corrections only.

References

[1] M. Chu *et al.*, "Respiration rate and volume measurements using wearable strain sensors," *NPJ Digit Med*, vol. 2, no. 1, pp. 1–9, 2019.

[2] L. Guo, L. Berglin, U. Wiklund, and H. Mattila, "Design of a garment-based sensing system for breathing monitoring," *Textile research journal*, vol. 83, no. 5, pp. 499–509, 2013.

[3] T. Ferkol and D. Schraufnagel, "The global burden of respiratory disease," *Ann Am Thorac Soc*, vol. 11, no. 3, pp. 404–406, 2014.

[4] T. Nurmagambetov, R. Kuwahara, and P. Garbe, "The economic burden of asthma in the United States, 2008–2013," *Ann Am Thorac Soc*, vol. 15, no. 3, pp. 348–356, 2018.

[5] G. B. Drummond, D. Fischer, and D. K. Arvind, "Current clinical methods of measurement of respiratory rate give imprecise values," *ERJ Open Res*, vol. 6, no. 3, 2020.

[6] M. W. Semler *et al.*, "Flash mob research: a single-day, multicenter, resident-directed study of respiratory rate," *Chest*, vol. 143, no. 6, pp. 1740–1744, 2013.

[7] R. O. Crapo, "Pulmonary-function testing," *New England Journal of Medicine*, vol. 331, no. 1, pp. 25–30, 1994.

[8] M. R. Miller *et al.*, "Standardisation of spirometry," *European respiratory journal*, vol. 26, no. 2, pp. 319–338, 2005.

[9] C. P. Subbe and S. Kinsella, "Continuous monitoring of respiratory rate in emergency admissions: evaluation of the RespiraSense™ sensor in acute care compared to the industry standard and gold standard," *Sensors*, vol. 18, no. 8, p. 2700, 2018.

[10] F. Q. AL-Khalidi, R. Saatchi, D. Burke, H. Elphick, and S. Tan, "Respiration rate monitoring methods: A review," *Pediatr Pulmonol*, vol. 46, no. 6, pp. 523–529, 2011.

[11] P. Corbishley and E. Rodriguez-Villegas, "Breathing detection: towards a miniaturized, wearable, battery-operated monitoring system," *IEEE Trans Biomed Eng*, vol. 55, no. 1, pp. 196–204, 2007.

[12] Y. Khan, A. E. Ostfeld, C. M. Lochner, A. Pierre, and A. C. Arias, "Monitoring of vital signs with flexible and wearable medical devices," *Advanced materials*, vol. 28, no. 22, pp. 4373–4395, 2016.

[13] N. A. Collop *et al.*, "Clinical guidelines for the use of unattended portable monitors in the diagnosis of obstructive sleep apnea in adult patients," *Journal of Clinical Sleep Medicine-JCSM*, vol. 3, no. 7, pp. 737–747, 2007.

[14] R. Farre, J. M. Montserrat, and D. Navajas, "Noninvasive monitoring of respiratory mechanics during sleep," *European Respiratory Journal*, vol. 24, no. 6, pp. 1052–1060, 2004.

[15] C. Massaroni *et al.*, "Optoelectronic plethysmography in clinical practice and research: a review," *Respiration*, vol. 93, no. 5, pp. 339–354, 2017.

[16] M. A. Sackner *et al.*, "Calibration of respiratory inductive plethysmograph during natural breathing," *J Appl Physiol*, vol. 66, no. 1, pp. 410–420, 1989.

[17] K. Konno and J. Mead, "Measurement of the separate volume changes of rib cage and abdomen during breathing," *J Appl Physiol*, vol. 22, no. 3, pp. 407–422, 1967.

[18] R. Wijesiriwardana, "Inductive fiber-meshed strain and displacement transducers for respiratory measuring systems and motion capturing systems," *IEEE Sens J*, vol. 6, no. 3, pp. 571–579, 2006.

[19] F. Carpi and D. De Rossi, "Electroactive polymer-based devices for e-textiles in biomedicine," *IEEE transactions on Information Technology in biomedicine*, vol. 9, no. 3, pp. 295–318, 2005.

[20] S. D. Min, Y. Yun, and H. Shin, "Simplified structural textile respiration sensor based on capacitive pressure sensing method," *IEEE Sens J*, vol. 14, no. 9, pp. 3245–3251, 2014.

[21] G. B. Drummond, D. Fischer, M. Lees, A. Bates, J. Mann, and D. K. Arvind, "Classifying signals from a wearable accelerometer device to measure respiratory rate," *ERJ Open Res*, vol. 7, no. 2, 2021.

[22] Y. Chen, P. Zhang, Y. Li, K. Zhang, J. Su, and L. Huang, "Flexible capacitive pressure sensor based on multi-walled carbon nanotubes microstructure electrodes," *J Phys D Appl Phys*, vol. 54, no. 15, p. 155101, 2021.

[23] A. Rohit and S. Kaya, "A Systematic Study of Wearable Multi-Modal Capacitive Textile Patches," *IEEE Sens J*, vol. 21, no. 23, pp. 26215–26225, Dec. 2021, doi: 10.1109/JSEN.2021.3059224.

[24] J. Lv *et al.*, "Multifunctional polypyrrole and rose-like silver flower-decorated E-textile with outstanding pressure/strain sensing and energy storage performance," *Chemical Engineering Journal*, vol. 427, p. 130823, 2022.

[25] S. Brady, L. E. Dunne, R. Tynan, D. Diamond, B. Smyth, and G. M. P. O'hare, "Garment-Based Monitoring of Respiration Rate Using a Foam Pressure Sensor," 2005. [Online]. Available: www.adaptiveinformation.net

[26] O. Atalay, W. R. Kennon, and E. Demirok, "Weft-knitted strain sensor for monitoring respiratory rate and its electro-mechanical modeling," *IEEE Sens J*, vol. 15, no. 1, pp. 110–122, 2014.

[27] C.-T. Huang, C.-L. Shen, C.-F. Tang, and S.-H. Chang, "A wearable yarn-based piezo-resistive sensor," *Sens Actuators A Phys*, vol. 141, no. 2, pp. 396–403, 2008.

[28] C. P. Subbe and S. Kinsella, "Continuous monitoring of respiratory rate in emergency admissions: evaluation of the RespiraSense™ sensor in acute care compared to the industry standard and gold standard," *Sensors*, vol. 18, no. 8, p. 2700, 2018.

[29] A. Ali *et al.*, "A Novel Wearable Sensor for Measuring Respiration Continuously and in Real Time," *Sensors*, vol. 24, no. 20, p. 6513, Oct. 2024, doi: 10.3390/s24206513.

[30] T. Hoffmann, B. Eilebrecht, and S. Leonhardt, "Respiratory monitoring system on the basis of capacitive textile force sensors," *IEEE Sens J*, vol. 11, no. 5, pp. 1112–1119, 2010.

[31] A. Rivadeneyra and J. A. López-Villanueva, "Recent advances in printed capacitive sensors," *Micromachines (Basel)*, vol. 11, no. 4, p. 367, 2020.

[32] N. Hayward *et al.*, "A capaciflector provides continuous and accurate respiratory rate monitoring for patients at rest and during exercise," *J Clin Monit Comput*, vol. 36, no. 5, pp. 1535–1546, 2022.

[33] J. M. Vranish, R. L. Mcconnell, and S. Mahalingam, "'CAPACIFLECTOR' COLLISION AVOIDANCE SENSORS FOR ROBOTS," 1991.

[34] J. M. Vranish, "Commercial Capaciflector," in *NASA, Washington, Technology 2001: The Second National Technology Transfer Conference and Exposition, Volume 2*, 1991.

[35] N. R. Lange and D. P. Schuster, "The measurement of lung water," *Crit Care*, vol. 3, pp. 1–6, 1999.

[36] Y. Xu, R. H. McQueen, M. Strickfaden, A. Aslund, and J. C. Batcheller, "Establishing thermal comfort: characterization of selected performance and physical properties of fabrics used in hospital operating room uniforms," *Journal of the Textile Institute*, vol. 103, no. 7, pp. 698–705, 2012.

[37] A. Ali, C. Smartt, J. Im, O. Williams, E. Lester, and S. Greedy, "Impact of dielectric substrates on chipless RFID tag performance," *Int J Microw Wirel Technol*, vol. 15, no. 5, pp. 753–763, Jun. 2023, doi: 10.1017/S1759078722001039.

[38] L. E. Dunne, S. Brady, B. Smyth, and D. Diamond, "Initial development and testing of a novel foam-based pressure sensor for wearable sensing," Mar. 01, 2005. doi: 10.1186/1743-0003-2-4.

[39] R. Kusche, F. John, M. Cimdins, and H. Hellbruck, "Contact-Free Biosignal Acquisition via Capacitive and Ultrasonic Sensors," *IEEE Access*, vol. 8, pp. 95629–95641, 2020, doi: 10.1109/ACCESS.2020.2995861.

Dr A. Ali completed his PhD degree in Electrical Engineering at the University of Nottingham, UK, in 2024. His research interest is in designing chipless RFID sensor tags for tracking the biomass supply chain, integrating smart materials to add sensing functionality for biomass humidity and temperature levels. He joined Nottingham Trent University as a research fellow in 2022 to design, simulate, and manufacture the respiratory rate sensor.

Dr Y. Wei is an Associate Professor in Department of Engineering at Nottingham Trent University and the lead of Smart Wearable Research Group which focuses on the development of innovative wearable solutions for a range of military and civilian applications. Dr Wei is also the academic lead of Smart Medical Textile at Medical Technologies Innovation Facility (MTIF), a £23M regional investment site on the NTU Clifton campus.

Dr Harry Akerman qualified as a Doctor from the University of London in 1997. In 2005 he was admitted as a fellow of the Royal College of Anaesthetists. Since 2015 he has been working with the school of Electronics and Computer Science at the University of Southampton and was awarded a Visiting Professorship in 2018. He is joint Chief Investigator and Clinical Lead on the NIHR i4i grant for the Capaciflector.

Neil M. White (Senior Member, IEEE) received the Ph.D. degree from the University of Southampton, Southampton, U.K., in 1988, for a thesis describing the piezoresistive effect in thick-film resistors.

He lectures on electronic circuits, MEMS and advanced instrumentation and sensors. He has co-authored several text books and has published more than 250 scientific articles in the area of sensors and energy harvesting systems. Professor White was the recipient of the 2009 Calendar Silver Medal, awarded by the Institute of Measurement and Control for his outstanding contribution to the art of instruments and measurement.

Dr. A. Jackson is an anaesthetic and intensive care doctor. Having trained at the University of Edinburgh, including a BMedSci in epidemiology, he moved to Southampton where he has pursued integrated clinical academic training. His primary research interest is the application of data science, including machine learning and artificial intelligence, to perioperative care. Sandy is passionate about making effective use of the growing wealth of healthcare data. To facilitate this, he has completed an MSc in Data Science and has been awarded an NIHR Doctoral Fellowship to support a PhD exploring patient-centred outcomes after major surgery.